CHARACTERIZATION OF COLD-REGIONS TERRAIN USING AIRBORNE LASER PROFILOMETRY

By W. D. HIBLER III

(U.S. Army Cold Regions Research and Engineering Laboratory, Hanover, New Hampshire 03755, U.S.A.)

ABSTRACT. This paper provides a review of the characteristics of airborne laser profilometry and its application to quantitative characterization of cold-regions terrain. The limitations of profilometry due to the profiler instrumental characteristics and instability of the aircraft platform (resulting from variations in aircraft altitude and attitude) are discussed. For typical aircraft speeds of the order of 100 m/s these limitations restrict the accurately measured roughness content to the approximate wavelength range 2 m to 300 m. Digital filtering and hardware techniques for removing the aircraft motion, and hence extending the long wavelength validity of the profile, are discussed.

Regarding terrain characterization, particular attenion is given to Arctic sea ice. Ridge height and spacing distribution models for sea ice in conjunction with digitally processed laser profiles allow efficient characterization of sea-ice ridging using only a few parameters. In particular, a single ridging intensity parameter has been found to allow reasonable estimation of the number of ridges encountered at any height level along a straight-line path. Examination of spectral characteristics of first-year and multi-year ice suggest that laser profiles may be used to identify the ice type of floes and ridges. Comparisons of laser data and submarine sonar data are made which suggest that ratios of *c.* 6.5 : 1 can be used to estimate ridge keel depths from laser data. Use of laser profilometry to characterize tundra and indirectly to measure variation in snow depth is briefly discussed.

RÉSUMÉ. *Caractérisation du terrain dans les régions froides par profilométrie aérienne au laser.* Cet article passe en revue les caractéristiques de la profilométrie aérienne au laser et de ses applications à un levé quantitatif du terrain dans les régions froides. Les limites de la profilométrie dûes aux caractéristiques instrumentales et à l'instabilité de la plateforme aérienne (variations de l'altitude et de l'attitude de l'avion) sont discutées. Pour des vitesses communes de l'avion de l'ordre de 100 m/s, ces limites restreignent la rugosité mesurée avec précision aux ondulations de l'ordre de 2 à 300 m. Un filtrage digital et des techniques électroméchaniques pour déterminer les mouvements de l'avion et par conséquent étendre la validité du profil dans les grandes longueurs d'onde font l'objet de discussions.

En ce qui concerne la caractérisation du terrain, une attention particulière est donnée à la glace de mer Arctique. La hauteur des crêtes de glace de mer et leur type de répartition dans l'espace, s'ajoutant à la digitalisation des profils au laser permet une caractérisation efficace des ondulations de la glace de mer en se servant d'un petit nombre de paramètres. En particulier, on a trouvé un paramètre unique pour l'intensité des ondulations de la glace de mer qui permet une estimation raisonnable du nombre de crêtes rencontrées à une altitude donnée le long d'un chemin rectiligne. L'examen des caractéristiques spectrales de glaces de première année et de glaces anciennes permet de penser que les profils laser peuvent être utilisés pour identifier le type de glace des glaçons flottants et des crêtes. En comparant les données au laser et les prospections sous-marines au sonar on pense qu'on peut utiliser un rapport d'environ 6,5 à 1 pour estimer la profondeur d'une quille sous-marine à partir des données du laser. On aborde brièvement l'utilisation de la profilométrie au laser pour caractériser la toundra et pour mesurer indirectement la variation de l'épaisseur de la neige.

ZUSAMMENFASSUNG. *Die Charakterisierung des Terrains in Kaltregionen mit Hilfe der Laser-Profilmessung aus der Luft.* Die Arbeit gibt eine Übersicht über die Kennzeichen der Laser-Profilmessung aus der Luft und deren Anwendung zur quantitativen Beschreibung des Terrains in Kaltregionen. Die Grenzen der Profilmessung infolge der instrumentellen Leistungsfähigkeit und der Instabilität der Anbringung im Flugzeug (hervorgerufen durch die Schwankungen der Flughöhe und -lage) werden diskutiert. Für typische Fluggeschwindigkeiten in der Grössenordnung von 100 m/s ist infolge dieser Grenzen der Messgenauigkeit für die Rauhigkeit der Oberfläche auf den Bereich von 2 bis 300 m beschränkt. Es wird dargelegt, wie sich durch digitale Filterung und Massnahmen zur Beseitigung der Flugzeugschwankungen die Zuverlässigkeit der langperiodischen Profilwerte erhöhen lässt.

Hinsichtlich der Terrainverhältnisse wird besonders auf arktisches Meereis eingegangen. Die Höhe der Meereisrücken und Modelle zu ihrer räumlichen Verteilung ermöglichen in Verbindung mit digital verarbeiteten Laser-Profilen eine zutreffende Charakterisierung der Rückenbildung im Meereis mit nur wenigen Parametern. Speziell ergab sich ein einziger Parameter für die Intensität der Rückenbildung, der eine vernünftige Abschätzung der Zahl jener Rücken erlaubt, die in einem bestimmten Niveau längs eines geraden Profiles anzutreffen sind. Die Prüfung der spektralen Verteilung in einjährigem und mehrjährigem Eis lässt erwarten, dass Laser-Profile zur Feststellung des Eistyps von Schollen und Rücken herangezogen werden können. Aus dem Vergleich von Laser- und Unterwasser-Sonardaten geht hervor, dass ein Verhältnis von 6,5 zu 1 zur Schätzung der Kieltiefe von Rücken aus Laserdaten benutzt werden kann. Die Benutzung der Laser-Profilmessung zur Charakterisierung der Tundra und zur indirekten Messung von Schneehöhenunterschieden wird kurz diskutiert.

INTRODUCTION

Laser profiling is a remote-sensing procedure in which the distance between an aircraft and the terrain surface is monitored at short time intervals in order to produce a record of the terrain elevation beneath the aircraft. Such profilers have been a useful addition to remote-sensing packages in aircraft since they supply a direct measure of the variations in surface topography. Although the laser profiler only supplies a record of variation in surface height along a straight-line path, such information is often adequate for specifying the nature of the surface roughness either by means of roughness spectral densities or by a description of the nature and distribution of discrete roughness elements. In addition to such direct measurements, profile data may be used indirectly to measure statistically certain parameters such as variations in snow depth, by flying profiles before and after snow fall.

Besides acquiring data only along a straight-line path, the primary limitations in profilometry data are due to (1) the finite response time and experimental error of the profiler and (2) instability in the aircraft platform due to variation in aircraft altitude and attitude. The finite response time means that very high-frequency roughness cannot be measured, whereas the platform instability limits the measurement of very low-frequency roughness.

In this paper we review and discuss both the basic characteristics and limitation of laser profile data, and also how such data can be used to characterize cold-regions terrain. In the review of limitations of the data we examine both (1) how the instrumental error and finite response time affect the profile and its spectral density and, (2) how digital and software processing techniques can be used to ameliorate the platform instability. In discussing the use of profile data to characterize terrains we will primarily discuss applications to sea-ice ridging and surface roughness, although application to tundra will be briefly mentioned.

CHARACTERISTICS AND LIMITATIONS OF PROFILOMETRY DATA

To understand the characteristics and limitations of airborne profilometry, it is convenient to compare the spectral densities of the actual terrain profile with those obtained by the profilometer. The spectral density of the laser trace will approximate the actual spectra closely over some frequency range, say f_1 to f_2. Frequences above f_2 will be smoothed and shifted in phase due to the finite instrument response time, whereas frequencies lower than f_1 will be partially spurious due to aircraft altitude and attitude variation. The cut-offs vary with the speed of the aircraft and the response time of the laser. In the valid frequency range f_1 to f_2 there will also be some spurious components due to distance error, which, as a first approximation, can be taken to be white noise (i.e. a random error) over this interval. The information from f_1 to f_2 will also be slightly modified by the attitude changes of the aircraft, which tend to change the effective speed of the pulse across the terrain surface. To examine in more detail the f_1, f_2 cut-offs we first discuss the characteristics of the profiler instrument which affect f_2.

Laser profiler characteristics

To obtain typical values for f_2, we consider a particular laser profiler, the "Geodolite 3A" which has been extensively used in sea-ice reconnaissance (see for example Ketchum, 1971) and also in land applications (Link, [1970]). This system is a typical continuous-wave laser profiler. Range measurements are accomplished through a phase comparison between the laser beam (with a modulated wave superimposed) directed at the terrain and the reflected light from the terrain. This phase difference is used to create a square wave with the tooth width proportional to the distance to the terrain surface modulo the superimposed wavelength (i.e. the tooth width is proportional to the distance less an integral number of wavelengths). This square wave is run through a simple integrating circuit whose output is an analog signal.

The integrating circuit smooths out distance errors (due to varying tooth widths) but has a finite response time and thus massages the high-frequency components. The response time is usually variable so one can trade off error reduction for a faster response time and vice versa. The available response times for the Geodolite 3A (defined as a 95% response to a step input) include 1, 2, 5, 10, 20, 50 and 100 ms. The modulation frequency is normally selected so that the phase delay of the reflected signal is one wavelength for a desired range change of 10 ft or 10 m depending on the particular instrument. Longer wavelengths may be chosen but they decrease accuracy. When this range interval is exceeded the indicated distance jumps back to zero and starts again. Such jumps are referred to as phase shifts.

Besides the range analog voltage, signal outputs from the laser include the photomultiplier output (return signal amplitude), which provides a means of distinguishing open-water areas from ice (when flying over lakes or sea ice) since signal return is quite low from open water.

Initial processing of the data involves removal of the phase shifts. The typical procedure is to digitize the analog signal at some high rate (200 samples per second) and then use simple algorithms to remove the phase shifts. Unfortunately phase discontinuities (range measurement errors caused by momentary loss of signal return) also occur occasionally. Such discontinuities are of varying magnitudes and usually require visual examination for identification and correction. The treatment of these kinds of instrumental peculiarities, although sometimes bothersome, is essentially a software problem which we will not discuss in further detail here. Additional discussion of this problem is given by Mock and others (1974).

Once the data is in an acceptable form with phase shift and discontinuities removed, we may examine how the response messages the data. Since the integrating circuit has essentially an exponential response, its frequency response $F(\omega)$ may be calculated straightforwardly:

$$F(\omega) = \beta \int_0^\infty \exp(-\beta t) \exp(i\omega t)\, dt = \frac{\beta(\beta+i\omega)}{\beta^2+\omega^2} \tag{1}$$

where by definition of the 95% response time Δt, $\beta = -\ln(0.05)/\Delta t$. In Figure 1 we give
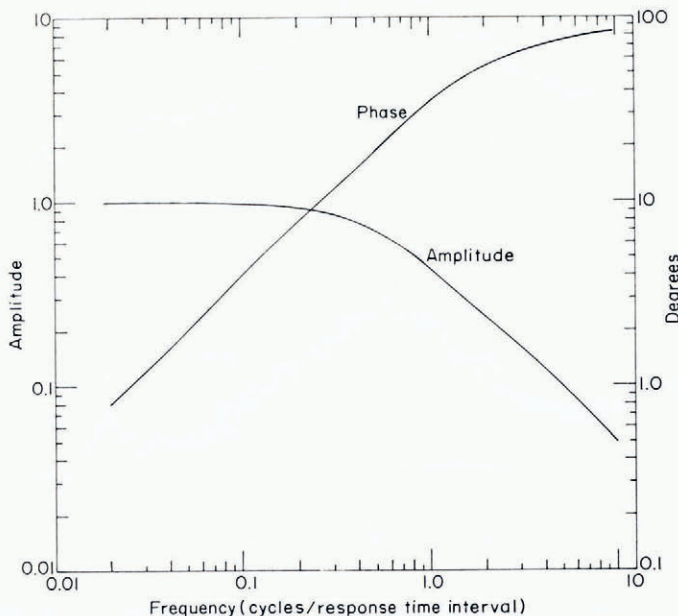

Fig. 1. Amplitude and phase of a causal exponential response function. The response time is defined as the time for a 95% response to a step input. Positive phase angles correspond to the output signal lagging behind the input signal.

a plot of the amplitude and phase of this response function with a positive phase angle indicating that the output signal is lagging in time behind the input. For conversion to distance, we note that 100 m/s (194.4 knots) is a typical aircraft speed, so that 10 ms corresponds to a 1 m distance. As can be seen from the figure, the high-frequency cut-off f_2, below which the data is modified little, is approximately 0.25 cycles/Δt. For a 10 ms response time and an aircraft speed of 100 m/s, this corresponds to a 4 m wavelength. This cut-off is close to the empirical wavelength cut-off of 6 m found by Tooma and Tucker (1973) in a comparison of laser–sea-ice profiles with aerial stereophotogrammetric profiles.

To examine the smoothing of the terrain profile by the profilometer plus the effect of noise more directly it is useful to filter some simulated terrain with exponential filters. The results of such a simulation are shown in Figure 2 where we have simulated a terrain by using
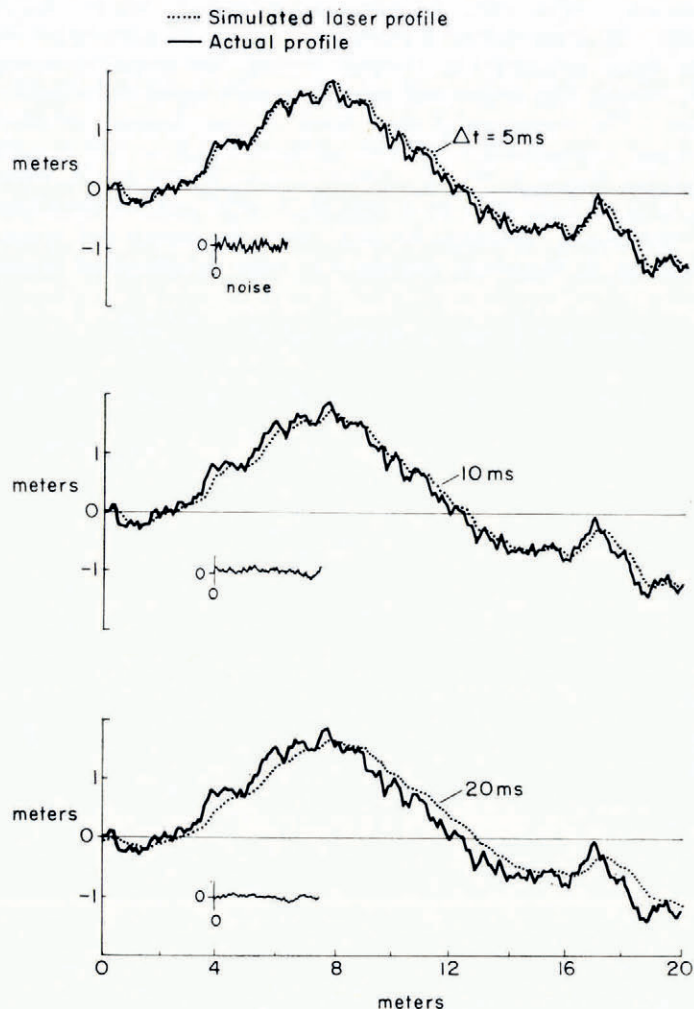

Fig. 2. *Results of filtering a simulated terrain profile with a causal exponential response function. An aircraft speed of 100 m/s (194.4 knots) was assumed. The noise was obtained by applying the various exponential filters to a fixed gaussian white-noise time series.*

a first-order Markovian process. Such a process has been found to have similar spectral characteristics to sea-ice profiles.

A nominal aircraft speed of 100 m/s is assumed. For the noise signal we used the fact that typical errors in sea-ice profiles (obtained by looking at the profile on flat ice) are of the order of 10 cm at a 10 ms response time (see for example Ketchum 1971, LeSchack and others, unpublished). These errors are somewhat smaller than the errors obtained from laser profile tests over land (Link, [1970]), which is to be expected because of the poor reflectivity over land.

As can be seen from the figure, the 5 ms and 10 ms responses modify the terrain only slightly, whereas the 20 ms smoothing begins to change phases and amplitudes significantly. The noise level on the other hand is moderately higher for the 5 ms response time, suggesting that 10 ms is a good compromise. We note that the effect of instrument response time on noise levels was studied empirically by Link ([1970]) with results similar to the simulation in Figure 2.

To summarize, the higher-frequency cut-off f_2 corresponds to wavelengths of the order of 2 to 4 m. Consequently, we may say that terrain that can be well described by samples every 1 or 2 m with height accuracy of few centimeters can be well characterized by aircraft profilometry. For more accuracy or a denser sampling rate, aircraft flying at speeds slower than c. 100 m/s would be needed. The price for this slower speed is a change in the low-frequency limit f_1, as discussed next.

Aircraft motion treatment

The variation of the altitude and attitude of the aircraft cause spurious low-frequency components to be present in the profile. Examples of this effect are shown in Figure 3 where two typical laser profile traces of sea ice are illustrated. The solid line is the estimated aircraft motion obtained according to a three-step digital filtering process discussed later (Hibler, 1972). The relevant observation here is that the aircraft motion causes variations of the order of 10 to 30 m with wavelengths greater than several hundred meters.

Various hardware devices have been proposed to handle the aircraft motion. The most common suggestions have been to use either a pressure-port calibrator and/or an accelerometer. The pressure-port method, although sensitive enough to resolve c. 0.15 m changes (Ketchum, 1971), is not highly useful because of horizontal variations in atmospheric pressure. To illustrate how great a problem this is, we note that vertical atmospheric changes are approximately 0.10 mbar/m (Berry and others, 1945). For an estimate of horizontal pressure
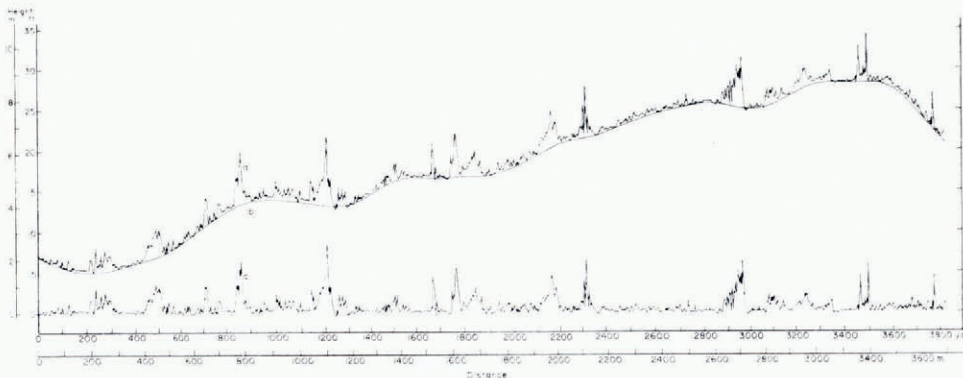

Fig. 3. Laser profile (curve a) of sea ice. Curve b represents the estimated variation in distance from the laser to the ice surface due to variation in aircraft altitude and attitude, and curve c is the result of subtracting b from a.

differences we calculated r.m.s. pressure differences between the three 1972 AIDJEX satellite stations located approximately 100 km apart, using pressure data reported by Thorndike and others (1972). For a 30 d period the r.m.s. differences averaged 0.016 mbar/km. This yields a height error of 0.16 m/km due to horizontal pressure variation, which is rather large especially for profiling Arctic sea ice.

The use of accelerometers appears to offer more promise although investigation of such data (personal communication from R. T. Lowry) indicates that they tend to drift slowly in time and thus cannot be used for the removal of extremely low-frequency height variations. A more complete discussion of the use of such data is given by Lowry (1975).

However, even if the aircraft altitude could be determined exactly, there still remains the problem of roll and pitch which also change the range to the terrain surface. For example a roll of $1°$ at a 320 m altitude causes a range change of c. 0.09 m. This sort of problem can be handled by using a gyro-stabilized gimbel mount but such systems are rarely employed.

Because of these difficulties it is more common to use digital filtering techniques. For purposes of spectral calculations one can simply use a variety of high-pass filtering techniques (see for example Hibler and LeSchack, 1972). Such a procedure is effective (and necessary) in preventing "leakage" of the low-frequency spectral components to higher frequencies. However, for other purposes such a procedure is not entirely adequate. This is because there is an overlap between the surface roughness spectrum and the aircraft motion spectrum. This overlap is especially troublesome in sea-ice profiles in that, as a consequence of the overlap, a high-pass filter tends to depress the height of high ridges.

To bypass this problem in sea ice a straight-forward three-step digital filtering process was developed by Hibler (1972). The technique consists of the following steps: (1) A symmetric high-pass convolution filter is applied to the initial profile. (2) From the filtered profile a set of minimum points are recorded; these minimum points are linearly interpolated and then (3) low-pass filtered to obtain an estimate of the aircraft motion. The aircraft motion is then subtracted from the initial profile and the resulting profile used for further analysis. The basis for this process is that the pack-ice surface profile is essentially a one-sided noise trace
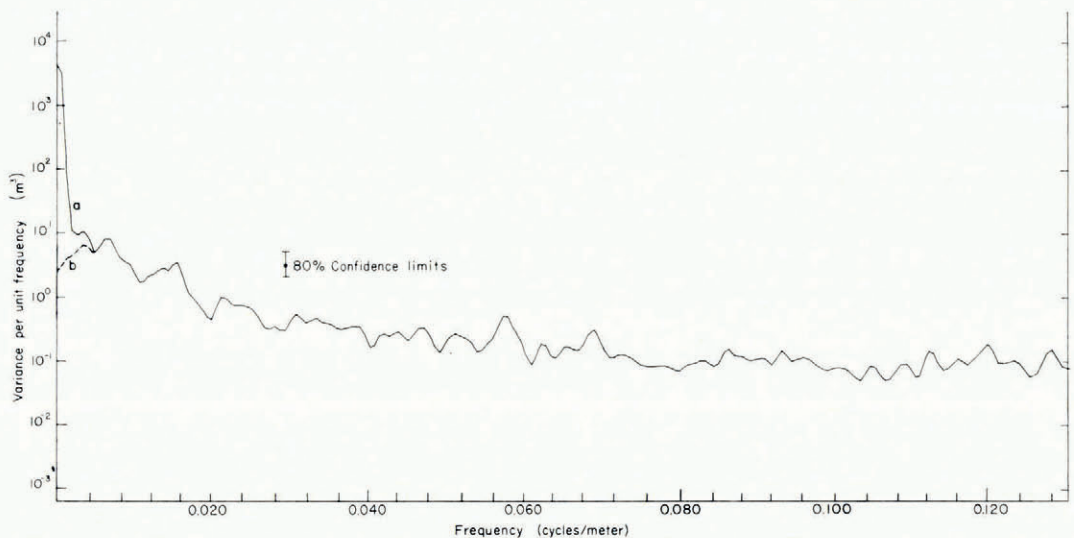

Fig. 4. *Power spectra of the filtered and unfiltered profiles shown in Fig. 3. Curve a is the unfiltered profile spectrum, and curve b is the spectrum of the profile after removal of aircraft motion.*

in that the roughness always rises up approximately from the water level. An example of this process is the smooth curve in Figure 3 which, as can be seen, provides an aircraft motion curve which is very close to what would be estimated visually.

It is also instructive to compare the low-frequency portion of the spectrum of the unfiltered profile and the profile with the aircraft motion removed. In Figure 4 we see such spectra corresponding to the profiles in Figure 3. The spectra clearly indicate the problem of spectral overlap. Although approximately 99% of the low-frequency variance is due to the aircraft motion, the residual 1% is significant on the scale of surface roughness. The spectra also indicate that the cut-off at which the unprocessed spectrum merges with the filtered spectrum occurs at a wavelength of about 240 m. This indicates that although the aircraft motion has most of its variance at very low frequencies, it also has a significant portion (on the surface roughness scale) at higher frequencies.

To summarize, for speeds of the order of 100 m/s, aircraft motion directly affects the spectrum at wavelengths larger than c. 300 m. If the profile is to be used to examine variation in roughness at wavelengths less than 300 m, the data may be used directly simply by low-pass filtering. If not, then some subterfuge must be used to push back the cut-off to lower frequencies. Also speeds faster or slower than 100 m/s will tend to move the f_1 cut-off lower or higher respectively.

CHARACTERIZATION OF COLD-REGIONS TERRAIN

Having examined the characteristics and limitations of laser data, we can now discuss its use for cold-region terrain classification. To this end we will primarily review the use of such data for characterizing sea-ice ridging and roughness in the Arctic Basin, although application to other terrains will be briefly mentioned.

Classification of sea-ice ridging

Sea-ice ridges are an important deformation characteristic of the Arctic ice pack and have been actively studied in the past several years. Results of this work have included studies of the morphological characteristics of ridges (Weeks and others, [1972]; Kovacs, 1972), the development of mechanical ridge-formation models (Parmerter and Coon, 1972); and the development of statistical models for describing the height and spatial distribution of pressure ridges (Hibler and others, 1972; Hibler and others, 1974). Laser profiles, in conjunction with the three-step filtering process, provide a means of rapidly compiling ridge height and spacing statistics along a straight-line path. Submarine sonar data, such as those discussed by Swithinbank (1972), provide similar information on the distribution of ridge keel depths. Such straight-line distribution data is especially useful in sea ice since it appears that over reasonably large areas (tens of kilometres) ridges are close to being randomly oriented in direction (Mock and others, 1972). Consequently the total length of ridges per unit area is related to the number of ridges encountered per unit length along a straight-line path.

In order to reduce the number of parameters needed to describe ridging statistically it is useful to develop height and spacing distribution models. Such a reduction is especially important when large quantities of data are being processed and it is desired to examine spatial and temporal variations in ridging. To derive a model for ridge height distributions Hibler and others (1972) carried out a variational calculation in which the most probable arrangement of a given number of ridges for a given amount of deformed ice (with no restriction placed on the maximum ridge height) was derived. The result in general form is given by:

$$P(H) \, dH = B(H) \exp(-\lambda H^2) \, dH \tag{2}$$

where $P(H) \, dH$ is the probability of finding a ridge with height between H and $H+dH$, and λ and $B(H)$ are to be determined. As a first approximation $B(H)$ was simply assumed to be

constant for H greater than some cut-off height h, a procedure which was found to yield adequate agreement with data above height h. Under this assumption Equation (2), when normalized to 1 for ridges above height h, becomes

$$P(H) \, dH = 2 \left(\frac{\lambda}{\pi}\right)^{\frac{1}{2}} \frac{\exp(-\lambda H^2)}{\operatorname{erfc}(\lambda^{\frac{1}{2}}h)} \, dH. \tag{3}$$

The key contribution of the variational calculation is the $\exp(-\lambda H^2)$ term in Equation (2). Additional assumptions can be made in the variational calculation that justify taking $B(H)$ as a constant (this was in fact done in the original paper by Hibler and others (1972)) but they tend to be oracular in nature. It is probably better to simply say that $B(H)$ being constant for $H > h$ is an empirical assumption that works reasonably well. A more detailed investigation with $B(H)$ varying as a function of height (or depth) could well be a subject for further research.

To illustrate the fit of Equation (3) as well as geographical variation in ridging, we show in Figure 5 three height distributions varying from heavily ridged ice near the northern Canadian Archipelago, to medium ridged ice near the North Pole and to lightly ridged ice in the Beaufort Sea. Each set of data was obtained from a laser track, $c.$ 40 km in length, with data spacings of 1.2 m to 1.5 m depending on the average aircraft speed. The total number of ridges above 4 ft (1.22 m) in each 40 km track varied from $c.$ 80 to $c.$ 400 ridges. Ridges were digitally identified by declaring a profile peak to be a ridge when the peak is at least 2 ft (0.61 m) above minimum points located both right and left of the peak. Seventy-eight other such 40 km samples have been fitted with Equation (3) with good agreement (Hibler and others, 1974).

As regards the spacing of ridges, the assumption that ridges occur randomly appears to be good. In particular, if ridges occur randomly, then their probability of occurrence is close to a Poisson distribution, which implies that the spacing distribution must necessarily contain a negative exponential, i.e. is of the form $B \exp(-\lambda L) \, dL$ where L is the spacing between ridge encounters. Such a distribution was found to fit spacing observation reasonably well (Mock and others, 1972). A factor of note here is that, if ridges are randomly oriented, then
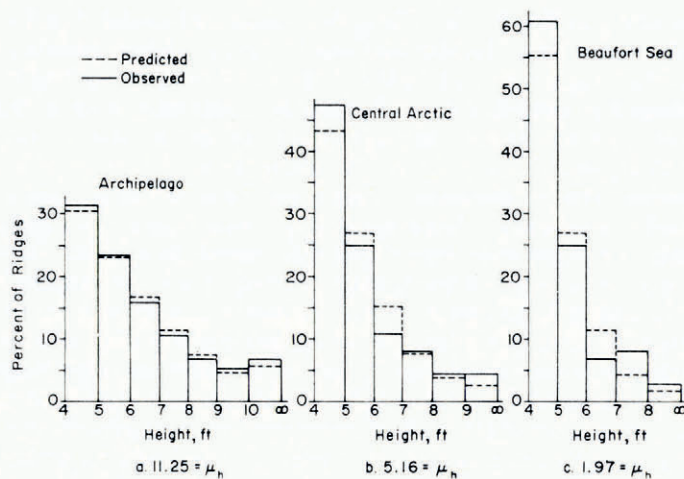

Fig. 5. *Ridge height distributions taken in February 1973. Each distribution was taken from a laser track approximately 40 km in length and the average number of ridges per kilometer above 4 ft (1.22 m) is denoted by μ_h for each distribution. The two-parameter fit is indicated by dashed lines with the actual data being solid. Distribution a, was observed at approximately lat. 83° N., long. 85° W., b at lat. 87° N., long. 162° W., c at lat. 70° N., long. 139° W. The mean ridge heights for distributions a, b and c were 1.93 m, 1.70 m, and 1.57 m respectively.*

μ_h, the number of ridges above height h per unit length along a straight-line path, is related to the total length of ridges per unit area above height h (called ridge density, R_h) by

$$R_h = (\pi/2)\,\mu_h. \tag{4}$$

It should be noted here that there are several different approaches to deciding if a profile peak is a ridge. An alternative procedure to the 2 ft (0.61 m) criterion (used for Figure 5) is to declare a peak to be a ridge when the minimum points are less than half of the peak height. This procedure has been used by Lowry (1975) and Williams and others (1975) and has been informally referred to by these authors as the "Rayleigh" criterion in analogy to optical signals. Comparison of these two procedures, using typical laser data, indicates relatively little difference in frequency of ridges above 4 ft (1.22 m), but pronounced differences for ridges below this height.

To illustrate these tendencies, we applied both techniques to the same data sets used in Figure 5. The results are shown in Figure 6. As can be seen, the Rayleigh procedure identifies somewhat fewer ridges above 4 ft (1.22 m) than the 2 ft (0.61 m) criterion. The effect varies from above 1% less for lightly ridged areas to about 10% less for heavily ridged areas with the percentages generally decreasing for the higher ridges. These results suggest that ridge statistics (for ridges >4 ft (1.22 m)) reported in Hibler and others (1974) would be changed only slightly by using the Rayleigh test. For ridges less than 4 ft (1.22 m), on the other hand, Figure 6 shows that the Rayleigh criterion yields many more ridges with the number of ridges with heights between 2 ft and 3 ft (0.61 m and 0.9 m) being anomalously large. Because of the difficulty of deciding what a small ridge really is (especially in rubble fields) these results suggest that probably the most reasonable approach for ridge identification is to use the Rayleigh criterion down to some cut-off greater than 1 m, and not to consider ridges lower than this.

Examination of Figure 5 together with the μ_h values (number of ridges per kilometer above height h) indicates a definite pattern in the shape of the distributions. In particular, the more ridges there are the greater the mean ridge height. Examination of a number of other distributions substantiated this effect and suggests that it might be possible, to some extent, to characterize both the ridge height and spacing distribution by a single parameter. In choosing
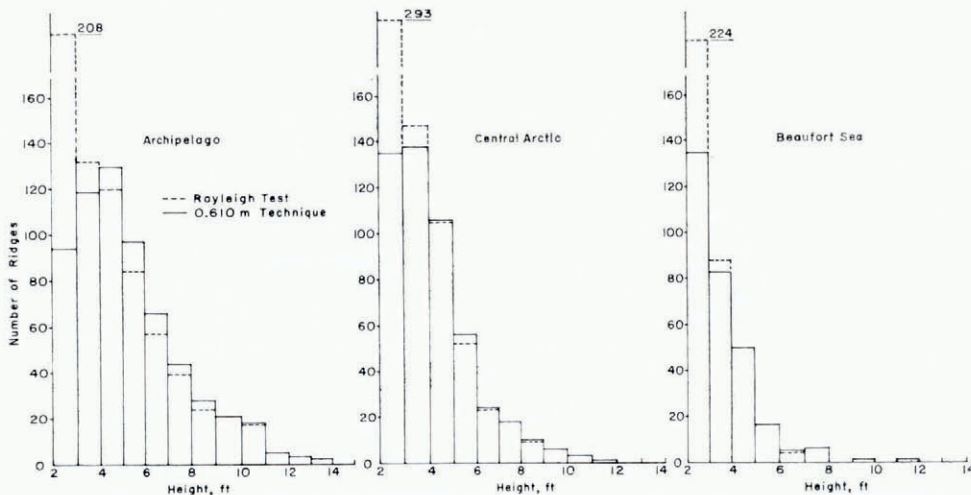

Fig. 6. *Comparison of ridge distributions obtained using the Rayleigh criterion, and the 2 ft (0.61 m) criterion.*

a single parameter for this purpose, common sense dictates that it should be some combination of the mean ridge height and mean ridge spacing. For this purpose, a parameter γ_h (called ridging intensity) defined by $\gamma_h \equiv \mu_h/\lambda$ has been found to describe ridging reasonably well (Hibler and others, 1974).

An example of the efficacy of such a one parameter model is given in Figure 7, which illustrates a plot of number of ridges per kilometer above 4 ft (1.22 m), 6 ft (1.83 m), and 8 ft (2.44 m) versus the square root of γ_h. The solid curves are constructed by an empirical procedure discussed by Hibler and others (1974). The data were taken from sixteen laser track samples each about 40 km long taken in November 1970. Figure 8 shows the geographical location and ridging intensity of each of the 16 samples along with rough contours of the ridging intensity. A discussion of the geographical, seasonal, and annual variations of ridging intensity using 81 such samples over the period November 1970 to February 1973 is given by Hibler and others, 1974. They also discuss the sampling stability of ridging parameters and conclude that the ridging intensity γ_h is a more statistically stable parameter than the mean ridge height or the mean ridge frequency μ_h.
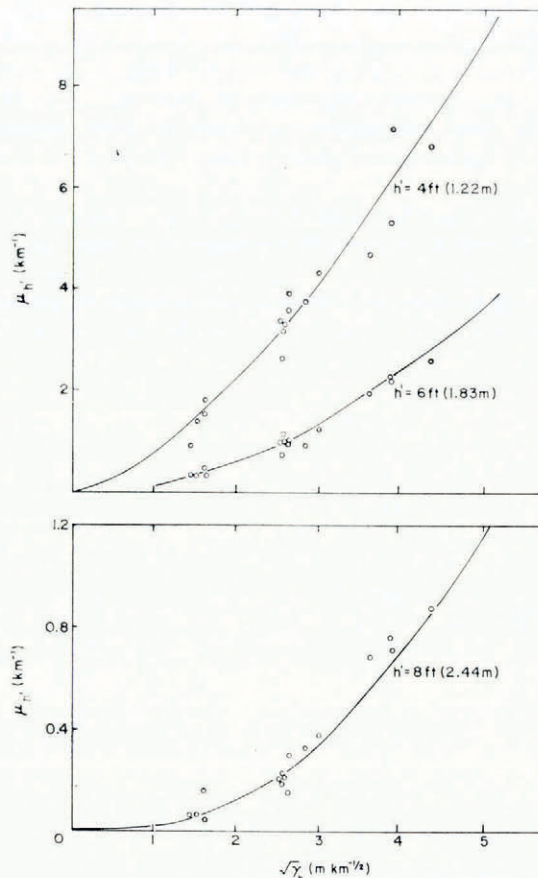

Fig. 7. Observed values (circles) for μ_h', the number of ridges per kilometer above height h', versus $\gamma_h^{\frac{1}{2}}$; $h = 4\,ft$ (1.22 m). The solid lines were constructed according to a procedure discussed by Hibler and others (1974). The observations were taken in November 1970 at locations illustrated in Figure 8.
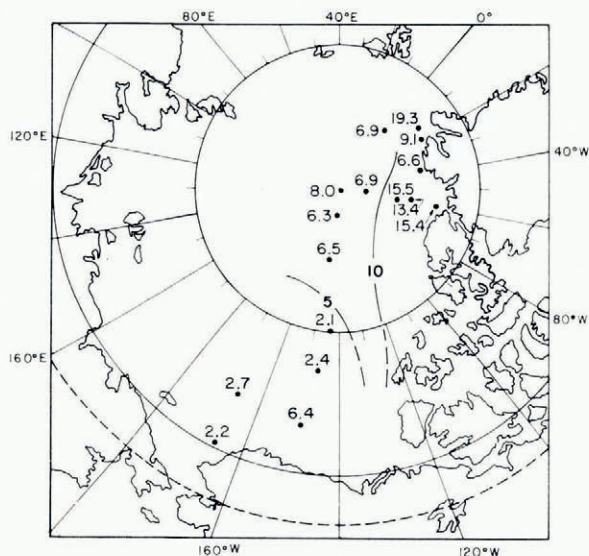
Fig. 8. Laser data sample locations and ridging intensities γ_h ($h = 1.22\ m$) for November 1970.

As a final point on ridge distribution models, we note that in some cases it may be useful simply to compile the ridge distributions empirically. The advantages of models are that they reduce the number of parameters necessary to characterize a given region and also supply an analytic functional form for other calculations such as wind form drag (see e.g. Arya, 1973). Also, in practice, there is some sampling instability so that e.g. two adjacent 40 km segments will have different statistics. Examination of the sampling error indicates that it is commensurate with the uncertainty in prediction from the one-parameter model so that for many purposes such a model offers adequate information to characterize ridging. In addition, it is conceptually useful to know that ridging is fairly well defined by a single parameter, since this means that if we can calculate, say, the volume of deformed ice from a sea-ice drift model, then the ridging characteristics can be estimated reasonably well.

Estimation of ridge keel depths

Besides characterizing ridge heights, laser data also provide an indirect measure of ridge keel depth distributions. For this purpose some relationship between keel depths and ridge heights is needed. Some data on this are available through measurement of individual ridges (Weeks and others, [1972]), but are too sparse to provide an adequate statistical sample. An indirect way to get keel to sail ratios is to compare height and depth percentage distributions in the same region and modify the height and depth scales until the two curves overlap. If Equation (3) is used to characterize the distribution, then it is easy to see that the probability density curves will coincide (within a constant factor) when the keel to height ratio is given by

$$\left(\frac{\text{keel}}{\text{height}}\right) = (\lambda_{\text{height}}/\lambda_{\text{keel}})^{\frac{1}{2}}. \qquad (5)$$

For a rough comparison of this type, submarine data from the 1960 winter cruise of the U.S.S. *Sargo* (see Hibler and others, 1972) yielded λ values of about 0.0117 m^{-2} near the North Pole and 0.0086 m^{-2} closer to the northern Canadian Archipelago. Typical laser data from the winter of 1971 (see Hibler and others, 1974) yielded λ values for similar regions of

0.517 m^{-2} and 0.357 m^{-2} which by Equation (4) gives ratios of 6.6 and 6.7. Comparison of laser data from winter 1973 would yield somewhat larger ratios. These ratios are larger than the 4.5 ratio observed by Kovacs (1972) in profiling individual ridges, but in the same range as the 7.6 ratio observed by Kan and others (1974) using sonar mapping and surface level lines. It should also be remembered here, that in data taken by Kovacs the ridge heights are generally taken to be the high points (or at least locations where the ridge is a well-defined obstacle) whereas the laser picks out whatever height it happens to go over, and there may well be a difference of several feet (a meter or two) between these measurements (Hibler and Ackley, 1973).

A graphical comparison of this type for laser and submarine sonar data has also been made in the East Greenland Sea by Kozo and Diachok (1973). They found that a ratio of five gave the best agreement. These results might indicate that the East Greenland Sea and Arctic Basin ratios are different. However, both these estimated ratios may be somewhat in error. The comparison made by Kozo and Diachok for example involved only 18 km tracks with relatively shallow ridges and no more than four class intervals in the distributions. On the other hand, the comparison of λ values, although taken from larger tracks and having more class intervals, were made in different years. Also, the comparison of percentage distribution makes no use of the spacing of ridges.

A more direct comparison which makes more complete use of the available information is to compare heights and depths where the same number of ridges per kilometer were encountered. Some data for this purpose were obtained during March 1971 near the North Pole. During this time both laser profile data (see Hibler and others, 1974) and submarine sonar data were acquired (Swithinbank, 1972; Williams and others, 1975). From these simultaneous data, we first obtained the number of ridge encounters (per km) at a given depth from the H.M.S. *Dreadnought* data between lat. 89° to 90° N. The laser data (using the one-parameter model with a characteristic γ_h) were used to determine heights where the same frequency of ridges was encountered. The results are shown in Figure 9. The solid line represents the regression line through the data and is given by $d = 6.58(h+0.17 \text{ m})$ (with a correlation coefficient of 0.99). Adding a small constant to the ridge height is reasonable since the three-step filtering process does not quite reduce the zero height to water level. The ratio of 6.58 is close to the ratio obtained earlier by taking λ values from different years.
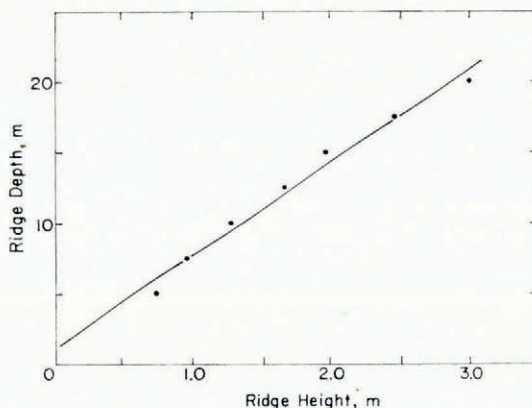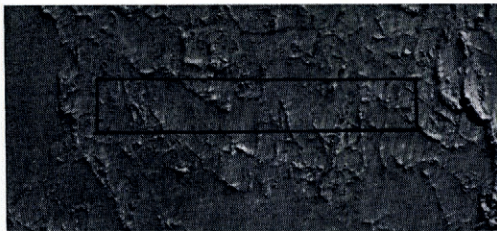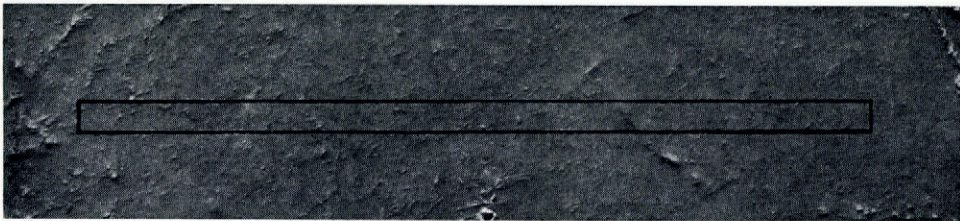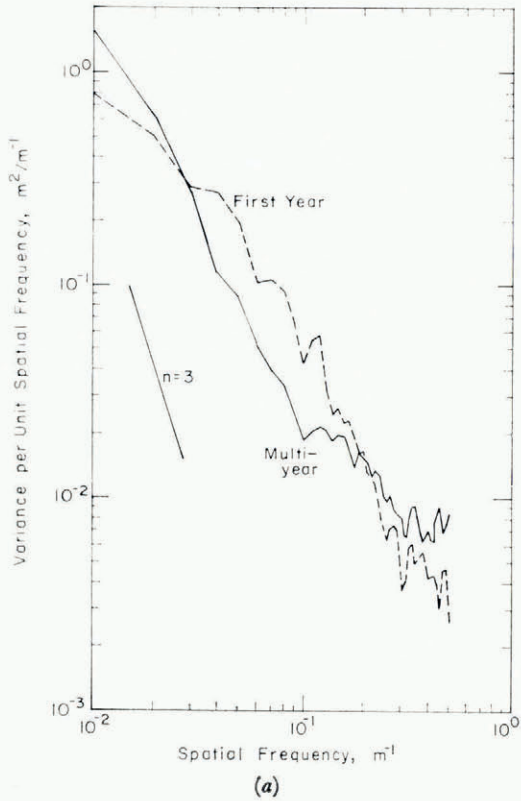

Fig. 9. Heights and depths at which the same number of ridges per kilometer were encountered. The data were taken near the North Pole in March 1971, and consisted of submarine data reported by Williams and others (1975) and laser data reported by Hibler and others (1974).

Fig. 10. Spectral densities (part a) of moderately rough first-year ice and relatively smooth multi-year ice calculated from stereophotogrammetric grids. Photographs showing the areas gridded are given in part b of the figure. Each spectrum represents the average of spectra along five parallel profiles 1 m apart. The average variances are 0.0335 m² and 0.0343 m² for the first-year and multi-year ice spectra respectively.

Spectral roughness characteristics of sea ice

Probably the most direct and simple terrain characterization that can be derived from the laser profiles is the spectral density. Spectral densities have traditionally been used to classify terrain surfaces for purposes of vehicular ride characteristics (Bekker, 1969, p. 319) and they serve a similar purpose for sea ice. The spectral approach also has certain other advantages in that it appears that spectral roughness may be usable to identify ice type (Hibler and LeSchack, 1972) and to estimate wind stress over relatively unridged ice (Banke and Smith, 1973).

To illustrate how spectral characteristics might be used to identify ice types we illustrate, in Figure 10, spectra of relatively flat multi-year and first-year ice. These spectra are calculated from height profiles made from stereo photos of multi-year and first-year ice as described by Mock and others (1974). As can be seen, the primary difference is that the first-year ice has somewhat more high-frequency roughness at wavelengths shorter than about 30 m. This difference suggests that an appropriate digital filter might be used to identify ice types.
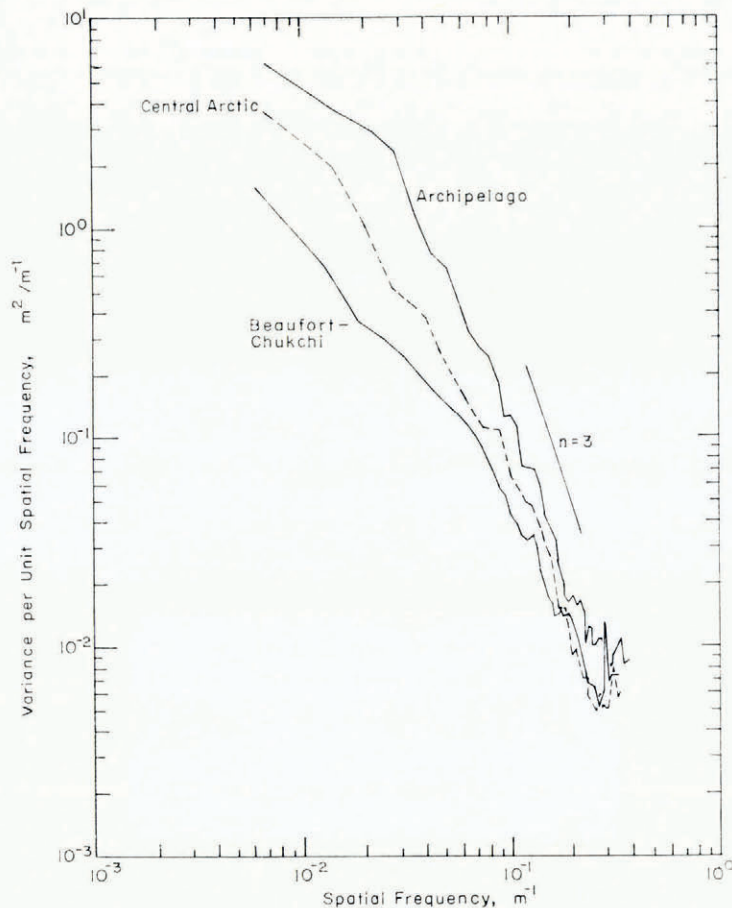

Fig. 11. *Spectral densities using laser profiles from three locations in Arctic Basin in November 1970. The spectra were each calculated from 4 000 data points and c. 1.4 m spacings. The ridging intensities for the tracks used were 15.4, 6.5 and 2.4 m²/km. Reference to Figure 8 using these ridging intensities allows identification of sample location.*

Examination of various sea-ice spectra indicates that the spectral density has geographical variations similar to those of ridging intensity. Some typical spectral densities shown in Figure 11 illustrate this effect. The spectral densities shown in this figure are taken from similar geographical regions as the ridge distributions in Figure 5. As can be seen, the slope of the double logarithmic spectral plots generally decrease as one proceeds from the heavily ridged region near the northern Canadian Archipelago to the more lightly ridged Beaufort Sea region. The slope of the double logarithmic plots lie between -2 and -3. The -3 slope is especially interesting, since, as noted by Nye (1973), such a slope is indicative of a terrain which "looks the same" at all scales.

To quantify the relationship between the spectral roughness of the sea ice and its ridging intensity it is useful to correlate the r.m.s. roughness parameter ζ_z, with γ_h, where ζ_z is defined by

$$\zeta_z{}^2 = \int_{+1/z}^{N_f} P(f)\, \mathrm{d}f, \tag{6}$$

N_f being the Nyquist frequency in cycles per meter and $P(f)$ the power spectrum. ζ_z thus represents the r.m.s. surface roughness at wavelengths shorter than z. To carry out the calculation of ζ_z, we used the first 4 000 data points from the 16 November 1970 samples. The lag product method with 200 lags and a Hamming spectral window was used to calculate $P(f)$, and ζ_z was calculated for $z = 13$ m and 200 m. Some of the results of these calculations are shown in Table I and Figure 12.

TABLE I. CORRELATION COEFFICIENT BETWEEN SPECTRAL AND RIDGE PARA-METERS

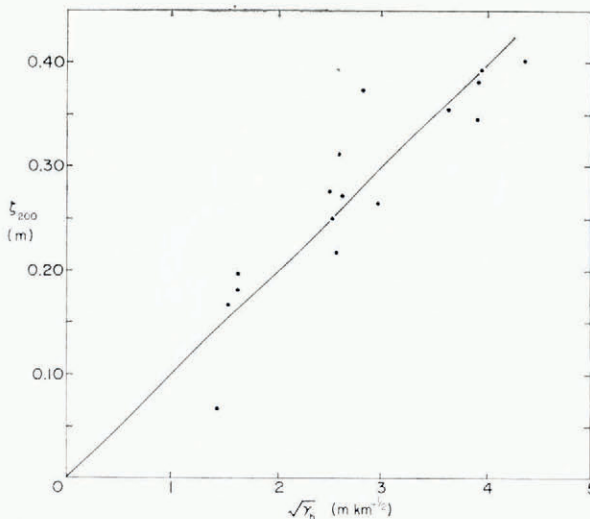|	$\gamma_h{}^{\frac{1}{2}}$	ζ_{200}	ζ_{13}
$\gamma_h{}^{\frac{1}{2}}$	1		
ζ_{200}	0.89	1	
ζ_{13}	0.82	0.92	1

Fig. 12. ζ_{200}, r.m.s. surface roughness for wavelengths less than 200 m, versus $\gamma_h{}^{\frac{1}{2}}$; $h = 4$ ft (1.22 m). The sample location (and γ_h values) are identified in Figure 8.

Figure 12 illustrates the high correlation between ζ_{200} and the square root of the ridging intensity. The least-squares line has the form $\zeta_{200} = m\gamma_h^{\frac{1}{2}}$ with $m = 0.0989$ km$^{\frac{1}{2}}$. Although not illustrated, a plot of ζ_{13} versus $\lambda_h^{\frac{1}{2}}$ shows a similar trend to that in Figure 12 with an m value of 0.0319 km$^{\frac{1}{2}}$. The implication of these results is that to a limited extent ridging intensity γ_h can be used to estimate spectral roughness as well as ridging.

Spectral characteristics of tundra

As discussed under the description of the laser profile data, when information on a given terrain in a frequency range 300 m to 2 m is desired, laser profilometry is useful. Tundra is an example of such a terrain, since it is commonly characterized by polygonal ground varying over lengths of several meters. Typical spectral densities of tundra before and after a snowfall are shown in Figure 13. The profiles for these spectra were made by hand at 0.5 m intervals. Examination of a number of other profiles besides this one (private communication from S. Mock) indicates that the spectral density is quite well described by $P(f) = \Omega f^n$ with n in the range -1.4 to -2.19 and log Ω varying from 0 to 0.64 (SI units used).

Work is underway to determine if this functional form can be extended to higher frequencies. If so, then laser profilometry would indirectly supply a measure of higher-frequency roughness characteristics, in that the spectral "window" from f_1 to f_2 could be used to estimate the parameters Ω and n.

Another dividend here is the similarity of summer-profile spectra and the snow-depth spectra. What has happened, of course, is that the snow has generally filled in the rapid
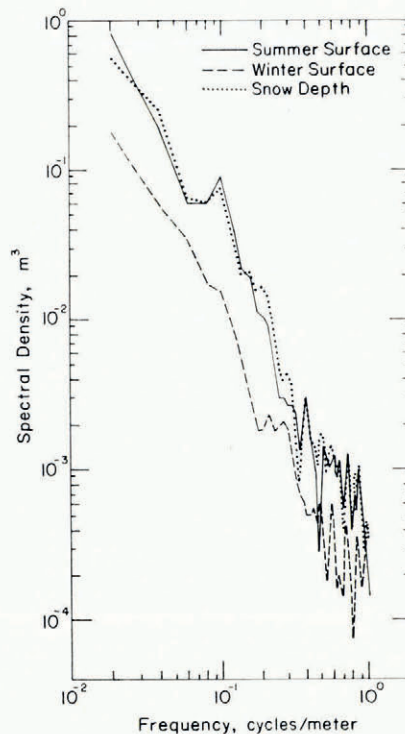

Fig. 13. *Tundra spectra of summer and winter profiles (taken at the same location) and snow depth. Each profile consisted of 260 points at 0.5 m spacings measured by spirit level before and after snowfall. The profile was located near Pt. Barrow, Alaska.*

terrain variations and thus the snow-depth spectrum is similar to the terrain profile spectrum. Coherence studies verify this and show the snow depth to be highly coherent with a phase shift of 180° as would be expected. This coherence does drop off at low frequencies however. Comparison of profiles before and after snowfall would allow some determination of this low-frequency cut-off and allow a statistical estimation of the variations in snow depth. Such information could be useful for water run-off studies, since a region with greater high-frequency roughness might trap more snow.

Conclusion

Past research has illustrated that airborne laser profilometry can be straightforwardly used to obtain statistical information about terrain roughness characteristics in a wavelength range from about 2 m to 300 m. Such a range is based on an aircraft speed of 100 m/s and would be shifted accordingly for different speeds. The profiles are useful for resolving discrete obstacles, but are not generally useful for direct measurement of small-scale roughness or very slow variations in terrain height.

Such profile data has proven especially useful for classification of sea-ice terrain, where the nature of the sea-ice surface allows processing of the data to determine ridge height and spacing distributions as well as spectral roughness characteristics automatically. Study of ridge characteristics show them to be reasonably well defined by one parameter, thus simplifying studies of regional and temporal ridging variations. Measurements of ridge heights can also be used to give a rough estimate of ridge keel depth characteristic for a given region.

REFERENCES

Arya, S. P. S. 1973. Contribution of form drag on pressure ridges to the air stress on Arctic ice. *Journal of Geophysical Research*, Vol. 78, No. 30, p. 7092–99.

Banke, E. G., *and* Smith, S. D. 1973. Wind stress on Arctic sea ice. *Journal of Geophysical Research*, Vol. 78, No. 33, p. 7871–83.

Bekker, M. G. 1969. *Introduction to terrain-vehicle systems.* Ann Arbor, University of Michigan Press.

Berry, F. A., *jr., and others.* 1945. *Handbook of meteorology, by F. A. Berry, Jr., E. Bollay and N. R. Beers.* New York, McGraw-Hill Book Co., Inc.

Hibler, W. D., III. 1972. Removal of aircraft altitude variation from laser profiles of the Arctic ice pack. *Journal of Geophysical Research,* Vol. 77, No. 36, p. 7190–95.

Hibler, W. D., III, *and* Ackley, S. F. 1973. Height variation along sea ice pressure ridges and the probability of finding "holes" for vehicle crossings. *U.S. Cold Regions Research and Engineering Laboratory. Special Report* 197.

Hibler, W. D., III, *and* LeSchack, L. A. 1972. Power spectrum analysis of undersea and surface sea-ice profiles. *Journal of Glaciology,* Vol. 11, No. 63, p. 345–56.

Hibler, W. D., III, *and others.* 1972. Statistical aspects of sea-ice ridge distributions, by W. D. Hibler III, W. F. Weeks and S. J. Mock. *Journal of Geophysical Research,* Vol. 77, No. 30, p. 5954–70.

Hibler, W. D., III, *and others.* 1974. Classification and variation of sea ice ridging in the western Arctic basin, [by] W. D. Hibler III, S. J. Mock and W. B. Tucker III. *Journal of Geophysical Research,* Vol. 79, No. 18, p. 2735–43.

Kan, T. K., *and others.* 1974. Sonar mapping of the underside of pack ice, [by] T. K. Kan, C. S. Clay and J. M. Berkson. *Journal of Geophysical Research,* Vol. 79, No. 3, p. 483–88.

Ketchum, R. D., *jr.* 1971. Airborne laser profiling of the Arctic pack ice. *Remote Sensing of Environment,* Vol. 2, No. 1, p. 41–52.

Kovacs, A. 1972. On pressured sea ice. (*In* Karlsson, T., *ed.* Sea ice. *Proceedings of an international conference.* ... *Reykjavik, Iceland, May 10–13, 1971.* Reykjavík, National Research Council, p. 276–95.)

Kozo, T. L., *and* Diachok, O. I. 1973. Spatial variability of topside and bottomside ice roughness and its relevance to underside acoustic reflection loss. *AIDJEX Bulletin,* No. 19, p. 113–22.

LeSchack, L. A., *and others.* Unpublished. Automatic processing of Arctic pack ice data obtained by submarine sonar and other remote sensing techniques, by L. A. LeSchack, W. D. Hibler III and F. H. Morse. [Technical report submitted to the Office of Naval Research under Contract N00014-70-C-0110 NR-307-322, September 1970.]

Link, L. E. [1970.] Capability of airborne laser profilometry system to measure surface roughness. *Proceedings of the sixth International Symposium on Remote Sensing of Environment . . . 1969. . . .* Ann Arbor, Willow Run Laboratories, Institute of Science and Technology, University of Michigan, Vol. 1, p. 189–96.

Lowry, R. T. 1975. An experiment in ice profiling in Nares Strait and the Arctic Ocean. *Journal of Glaciology,* Vol. 15, No. 73, p. 462–63. [Abstract.]

Mock, S. J., *and others.* 1972. Spatial aspects of pressure ridge statistics, [by] S. J. Mock, A. D. Hartwell and W. D. Hibler III. *Journal of Geophysical Research,* Vol. 77, No. 30, p. 5945–53.

Mock, S. J., *and others.* 1974. Arctic terrain characteristics data bank, by S. J. Mock, V. LeGarde and W. B. Tucker III. *U.S. Cold Regions Research and Engineering Laboratory. Technical Report* 247.

Nye, J. F. 1973. A note on the power spectrum of sea ice profiles. *AIDJEX Bulletin,* No. 21, p. 20–22.

Parmerter, R. R., *and* Coon, M. D. 1972. Model of pressure ridge formation in sea ice. *Journal of Geophysical Research,* Vol. 77, No. 33, p. 6565–75.

Swithinbank, C. W. M. 1972. Arctic pack ice from below. (*In* Karlsson, T., *ed. Sea ice. Proceedings of an international conference. . . . Reykjavík, Iceland, May 10–13, 1971.* Reykjavík, National Research Council, p. 246–54.)

Thorndike, A. S., *and others.* 1972. Station positions, azimuths, weather, 1972 AIDJEX pilot study. Preliminary data, by AIDJEX staff, by A. S. Thorndike, P. Martin, D. Bell, I. Virsnieks and A. Gill. *AIDJEX Bulletin,* No. 14, p. 63–71.

Tooma, S. G., *jr., and* Tucker, W. B., III. 1973. Statistical comparison of airborne laser and stereophotogrammetric sea ice profiles. *Remote Sensing of Environment,* Vol. 2, No. 4, p. 261–72.

Weeks, W. F., *and others.* [1972.] Pressure ridge characteristics in the Arctic coastal environment, by W. F. Weeks, A. Kovacs and W. D. Hibler III. (*In* Wetteland, S. S., *and* Bruun, P., *ed. Proceedings, the first international conference on port and ocean engineering under Arctic conditions., the Technical University of Norway, Trondheim, Norway, Aug. 23–30, 1971.* Trondheim, Technical University of Norway, Vol. 1, p. 152–83.)

Williams, E., *and others.* 1975. A submarine sonar study of Arctic pack ice, by E. Williams, C. [W. M.] Swithinbank and G. de Q. Robin. *Journal of Glaciology,* Vol. 15, No. 73, p. 349–62.

DISCUSSION

S. G. Tooma: Have you attempted to remove the errors produced by the other aircraft motions of pitch, roll, and crabbing? If not, do you have any ideas as to how this can be done?

W. D. Hibler III: The three-step filtering process does effectively take out all distance variations, including those caused by pitch and roll. I have not, however, made any attempt to employ hardware to remove these effects. I think that any successful procedure of accurately removing pitch and roll (and for that matter, altitude variations) will involve a combination of hardware devices and digital processing of the laser profile trace. As an example, you might use an integrated accelerometer trace to replace the first digital filtering operation in the three-step filtering process. This would greatly improve the aircraft-motion-removal procedure while simultaneously obviating the accelerometer drift problem.

E. R. Pounder: Were any of the correlations between ridge height and keel depths based on top and bottom profiles over the same traverse? What is the present limit on getting absolute ridge heights (above m.s.l.) from laser data?

Hibler: The correlation between the ridge heights and keel depths illustrated in the paper employed heights and depths in the same geographical region, month (March), and year (1971), but not from profiles on the same traverse. As regards absolute ridge heights, they are simply measured from the estimated ice surface which is typically several centimeters above the water level. From examining processed profiles the error in ridge heights using these processing techniques appears typically to be 10 cm and may be as large as 40 cm.

J. F. Nye: While the leads in sea ice represent the tensile deformation that has occurred very recently (days or weeks previously), the ridges represent several years of accumulated history of compression events. For studies of deformation it is therefore very desirable to be able to distinguish the fresh ridges from the old ones. Do you think your type of technique could have enough resolving power to see the difference?

HIBLER: It may well be possible to distinguish ridges that have been through at least one melt season from ridges that have not. This could in principle be effected by looking at the spectral roughness characteristics. I do think this approach has merit, but further study is necessary to establish the reliability and limitations.

W. F. WEEKS: I think the fact that Dr Hibler is thinking of using laser data to estimate the thickness of sea ice by determining the ice freeboard, gives ample testimony to exactly how desperately we need a direct method for determining sea-ice thickness.